Supplemental Data File

Perineuronal net degradation rescues CA2 plasticity in Rett syndrome model mice

Kelly E. Carstens, Daniel J. Lustberg, Emma Shaughnessy, Katharine E. McCann, Georgia M. Alexander, and Serena M. Dudek

Methods

Animals: Animals in all experiments were housed under a 12:12 light/dark cycle with access to food and water *ad libitum*. No specific method was used to randomize subject mice and were chosen arbitrarily for experiments. Animal numbers were pre-determined using an *a priori* power analysis seeking 90% power with an alpha level of 0.05. A limited number of post-hoc analyses were performed with alpha set to 0.05, and power was found to be >95% in CA2 of *Mecp2*$^{-/y}$ vs. WT at all ages. The experimenter was blinded to *Mecp2* genotype in all experiments.

Rett Syndrome mouse model: Mice used in this study were hemizygous MeCP2-deficient males (*Mecp2*$^{-/y}$; B6.129P2(C) -Mecp2$^{tm1.1Bird}$ via The Jackson Laboratory, stock # 003890, donated by Adrian Bird, University of Edinburgh (1)). *Mecp2*-null mutant males exhibit severe RTT-like characteristics at 3-8 weeks of age, whereas heterozygous females exhibit symptoms much later, around 6 months of age (2). This mouse line was maintained by breeding heterozygous *Mecp2*$^{-/x}$ females with C57BL/6 males. No special breeding conditions were used.

CA2 Cre-expressing line: To gain selective genetic access to molecularly-defined CA2, we used an *Amigo2-Cre* line that expresses Cre recombinase predominantly in CA2 neurons in adult mice. The *Amigo2-Cre* mouse line was generated in house at the NIEHS (3). The *Amigo2* gene (adhesion molecule with Ig like domain 2) is expressed in CA2/3a, the fasciola cinereum, the cerebellum, the accessory olfactory bulb, and the premammillary nucleus. This mouse was generated from a bacterial artificial

chromosome (BAC) transgene (Rp23-288P18); as in *Tg(Amigo2-EGP)LW244Gsat*2 (GENSAT[1]) (6). *Amigo2-cre* mice were maintained as hemizygous by breeding *Amigo2-Cre*+ mice with C57BL/6 mice. Only Cre^{+} males were used in this study and brains harvested >3 weeks old.

Conditional deletion of MECP2: For deletion of MeCP2 in CA2 pyramidal neurons, we used commercially available mice with an X-linked mutation, *loxP* sites flanking exons 3-4 of the *Mecp2* gene (floxed-*Mecp2*; $Mecp2^{flox}$; B6.129P2(C) -$Mecp2^{tm1.1Bird}$/J) via the Jackson Laboratory, stock # 006847, donated by Adrian Bird, University of Edinburgh (1)). This mouse line was maintained by breeding heterozygous $Mecp2^{flox/x}$ with C57BL/6 males; the hemizygous males $Mecp2^{flox/y}$ are infertile. To delete MeCP2 in CA2 neurons, we crossed heterozygous floxed-*Mecp2* females with *Amigo2-*Cre^{+} males. *MeCP2* is excised upon the recombination of the *loxP* sites in neurons expressing Cre recombinase. Tissue was harvested at P45 from the offspring *Amigo2-Cre+*; $Mecp2^{flox/y}$ and from 3 control groups: *Amigo2-Cre-*; $Mecp2^{WT/y}$, *Amigo2-Cre-*; $Mecp2^{flox/y}$, *Amigo2-Cre+*; $Mecp2^{WT/y}$.

Conditional CA2 Cre-expression line: To gain selective genetic access to molecularly-defined CA2 for DREADD experiments, we generated a tamoxifen-inducible mouse line, *Amigo2*-icreERT2. Expression of Cre in CA2 was validated by crossing *Amigo2*-icreERT2+ with a Cre-dependent tdTomato reporter mouse line (7). Mice expressed tdTomato in CA2 of *Amigo2-icre*ERT2+; *ROSA*-tdTomato+/- treated with tamoxifen (see Figure S1 of Alexander et al. (2017) for expression of the Cre indicator (3, 4)). The localization to CA2 pyramidal neurons was characterized by co-labeling with the CA2 pyramidal cell marker, PCP4, and an inhibitory neuron marker, GAD. The expression of Cre was indeed localized to CA2 pyramidal neurons and not inhibitory neurons in the hippocampus.

Epilepsy mouse model: Kv1.1-null mouse (also known as *Kcna1* knock-out mouse), C3HeB.129S7-*Kcna1*^{tm1Tem}/J via The Jackson Laboratory, stock # 003532, donated by Bruce L. Tempel, University of

[1] The Gene Expression Nervous System Atlas (GENSAT) Project, NINDS Contracts N01NS02331 & HHSN271200723701C to The Rockefeller University (New York, NY).

Washington School of Medicine (8). We crossed heterozygous Kv1.1$^{+/-}$ mice and used homozygous male and female Kv1.1$^{-/-}$ knock-out mice to measure *in vivo* electrophysiology and to quantify PNN staining.

Immunostaining (human brain): Human brain tissue was obtained from the NIH NeuroBioBank (https://neurobiobank.nih.gov). The RTT tissue was obtained from an individual clinically diagnosed with RTT: female age 20 years. The control tissue was from an age- and gender-matched, non-RTT individual, female age 19 years. Sections were cut at 8-µm on a sliding microtome. For the HAPLN1 staining, formalin-fixed paraffin-embedded human brain sections were deparaffinized and rehydrated through graded alcohols. Heat induced antigen retrieval was performed using a 1X citrate buffer solution, pH 6.0 (Biocare Medical, Concord, CA) in the Decloaker® pressure chamber for 15 minutes at 110° C, followed by 3% H_2O_2 to quench endogenous peroxidase activity. Non-specific binding was blocked with 10% normal donkey serum (Jackson Immunoresearch, West Grove, PA) and the avidin/biotin blocking kit (Vector Laboratories, Burlingame, CA). Sections were incubated with goat polyclonal anti-HAPLN1 antibody (R&D Systems, Minneapolis, MN, Cat# AF2608, Lot# VBN0218102) at 1:500 for 1 h at room temperature. Sections were then incubated with biotinylated donkey anti-goat IgG (Jackson Immunoresearch) at a 1:500 dilution. The antigen-antibody complex was detected using Vectastain Elite ABC R.T.U. label (Vector Laboratories, Burlingame, CA) and 3,3-diaminobenzidine (DAB) (Dako, Carpinteria, CA). Slides were then counterstained with hematoxylin, dehydrated and coverslipped. Slides were imaged using the slide scanner Aperio AT2 Scanner (Aperio: Leica Biosystems Inc.), which uses line scanning technology to capture high resolution digital images. Images were viewed and captured using Aperio ImageScope v. 12.3.0.5056 (Aperio: Leicca Biosystems Inc).

For the RGS14 staining, endogenous peroxidase was blocked using 3% H_2O_2. Heat-induced epitope retrieval was performed using a 1X EDTA buffer solution, pH 8.5 (Biocare Medical, Concord, CA) in the Decloaker® pressure chamber for 15 minutes at 110° C. Non-specific sites were blocked using

10% normal donkey serum (Jackson Immunoresearch) for 20 minutes at room temperature. Next, the sections were incubated with avidin/biotin blocking kit (Vector). The sections were then incubated in rabbit polyclonal RSG14 antibody (Proteintech, Rosemont, IL, Cat# 16258-1-AP, Lot# 48839, 0.47 mg/ml) at a 1:500 dilution for 60 minutes at room temperature. Normal Rabbit IgG Isotype Control (Calbiochem, Temecula, CA, Cat# NI01, Lot# 2659621, 0.1 mg/ml) at the equivalent dilution of 1:100 was applied to the negative control. Secondary incubation was done by using a biotinylated donkey anti-rabbit IgG antibody (Jackson Immunoresearch, Cat# 711-065-152, Lot# 138799) at a dilution of 1:500 for 30 minutes at room temperature. Further, the sections were incubated with R.T.U. Vectastain Kit (Vector) for 30 minutes at room temperature. The antigen-antibody complex was visualized using DAB chromogen for 6 minutes at room temperature. Finally, the sections were counterstained with hematoxylin, dehydrated through graded ethanol, cleared in xylene, and coverslipped.

Immunostaining (mice)**:** Mice were deeply anesthetized with Fatal-Plus (sodium pentobarbitaol, 50 mg/mL; >100 mg/kg intraperitoneal (IP) injection) and perfused with cold phosphate-buffered saline (PBS), followed by 4% paraformaldehyde in PBS (pH 7.4). Brains were removed and post-fixed overnight at 4°C and submerged in 30% sucrose. Forty-µm thick sections were cut on a sliding microtome, blocked in 5% normal goat serum and incubated in biotin-conjugated WFA lectin (Sigma Aldrich L1516, 1:1000), or rabbit anti-MECP2 (07-013, Millipore, 1:500), or mouse anti-regulator of G-protein signaling 14 (RGS-14) (UC Davis/NIH NeuroMab Facility, AB_10698026, 1:500), or rabbit anti-PCP4 (Invitrogen, AB 2645298, 1:500) overnight at 4^0 C. Sections were washed 3 times in PBS and incubated in secondary antibody at 1:500 for 40 minutes at room temperature: streptavidin Alexa-568, or goat anti-rabbit H+L A-568, or goat anti-mouse Alexa-568, or goat anti-rabbit Alexa-568 (Invitrogen). Sections were mounted with Vectashield anti-fade mounting medium with DAPI (Vector laboratories). Images were acquired on a Zeiss AxioObserver Z1 fluorescence microscope (Carl Zeiss Inc, Oberkochen, Germany). Stains were

visualized with Zeiss filterset 49 (335-383 nm excitation, and 420-470 nm emission), Zeiss filterset 38 (450-490 nm excitation, and 500-550 nm emission), or Zeiss filterset 43 (538-562 nm excitation, 570-640 nm emission) using a Zeiss AxioCam MR R3 camera.

Fluorescence intensity was quantified using FIJI software (9). To analyze WFA fluorescence intensity, all sections were processed and imaged concurrently and exposure settings on the epifluorescence microscope were maintained across images. To quantify fluorescence intensity in hippocampal subregion CA2, a contour was drawn around CA2 cells in the stratum pyramidale layer using the CA2 pyramidal cell marker, PCP4, as a guide. The 'mean gray value' of WFA fluorescence was measured inside the contour. The same protocol was followed to measure RGS14 fluorescence intensity in CA2. To analyze WFA-expressing cells in hippocampal subregion CA1 and CA3, a contour was drawn around five WFA+ cell bodies in each subregion and 'mean gray value' was measured and averaged in each subregion. To analyze WFA fluorescence intensity in overlying somatosensory cortical region, a fixed contour was positioned over layer 2/3 and 'mean gray value' was measured. Statistical analyses were performed using Graph-Pad Prism 8.0 software; significance was calculated using an α level of 0.05.

For brightfield images of biotinylated-WFA, sections were incubated in peroxidase blocking (0.3% H_2O_2 in methanol) for 10 minutes at room temperature, washed and then incubated in biotinylated-WFA overnight at 1:500. Sections were washed and incubated in ABC-peroxidase solution (Vector lab PK-6100) for 30 minutes at room temperature, washed again. Staining was detected by DAB substrate using the Peroxidase Substrate DAB kit (Vector SK-4100) and following the kit protocol. Sections were washed and mounted in Permount (Fisher). Images were scanned using the Aperio AT2 Scanner (Aperio: Leica Biosystems Inc) and viewed/ captured using the Aperio ImageScope v. 12.3.0.5056 (Aperio: Leica Biosystems Inc).

NanoString: Mice at P10 and P18 (N=3 males at P10, N=4 males at P18, WT and *Mecp2*-null per group) were anesthetized with Fatal Plus as above and brains were quickly harvested on ice in an RNase-free environment. A sagittal cut was made to separate the two hemispheres. Each hippocampus was dissected free and the ventral one-third (approximate) was removed and not used, as many CA2 enriched genes are not expressed in the ventral hippocampus. Hippocampal tissue was immediately frozen on dry ice and stored at -80°C for subsequent processing. RNA was extracted using the Qiagen RNeasy Mini Kit (Germantown, MD), and the concentration of each sample was measured using a nanodrop spectrophotometer. mRNA levels were determined using the NanoString (www.nanostring.com) platform utilizing a previously published custom code set from our lab that included CA2-enriched genes and hippocampal plasticity-regulating genes (86). CA2-enriched genes were selected from the results of a RNA-sequencing analysis from our lab that determined CA2 gene enrichment using laser capture microdissection of the cell body regions of CA1, CA2, CA3 and dentate gyrus (12). 100ng of each total RNA sample was prepared as per the manufacturer's instructions. RNA expression was quantified on the nCounter Digital Analyzer and raw and normalized counts were generated with nSolver (v4.0) software. Data were normalized utilizing the manufacturer's positive and negative experimental control probes, as well as 3 housekeeping genes with low %CV and that were representative of the range intensity of the endogenous data (*Alas1*, *Gapdh*, and *Ywhaz*). All samples passed nSolver's initial QA/QC controls. All replicates were very well correlated ($R > 0.98$). Normalized data ($\log_2$ of counts) were imported into Partek (St. Louis, MO) and quantile normalized for further QA/QC and statistical analyses. To identify significant differences in RNA expression, a *t*-test on treatment groups was performed with post-hoc Benhamini-Hochberg false discovery rate for each group comparison.

Immunoblotting: As described above, the *Mecp2*-null or WT littermate males (P45-60) were deeply anesthetized with Fatal Plus and brains were quickly harvested on ice. A sagittal cut was made to separate the two hemispheres and the ventral one-third (approximate) of the hippocampus was removed. Hippocampal hemispheres were lysed with RIPA buffer (Thermo) with Halt™ protease/phosphatase inhibitor cocktail (Thermo). Lysate was briefly sonicated and incubated on ice for 30 minutes while rocking. The lysate was centrifuged and resolved by gel electrophoresis and transferred to a nitrocellulose membrane using the iBlot gel transfer apparatus (Invitrogen). Immunoblots were incubated with primary antibody overnight, washed 3X in PBS with 0.01% Tween for five minutes each and incubated in secondary for two hours. They were again washed 3X in PBS with 0.01% Tween for five minutes each. Blots were visualized with an Odyssey infrared scanner (Li-COR Biosciences) after immunolabeling primary antibodies with infrared fluorophore–tagged secondary antibody (LiCor). Images were analyzed using the ImageJ; the mean gray value of the band of interest was measured and background was subtracted (defined as a region in close proximity to the band of interest).

Equal amounts of protein (25 µg) from each sample were loaded on 4-12% bis-tris NuPage gels (Invitrogen) and transferred to nitrocellulose membranes. The following antibodies were used: rabbit antibody to MMP-9 (PA5-13199, Invitrogen, 1:1000) antibody to β-actin (MA5-15739, Invitrogen, 1:10,000), donkey secondary antibody to rabbit IgG IRDye680RD® (925-68073, LiCor, 1:500), and goat secondary antibody to mouse IgG (H+L) IRDye800CW® (924-32210, LiCor).

In vitro electrophysiology: Mice (Charles River Laboratories, Raleigh, NC or bred in house) were deeply anesthetized with Fatal-Plus, decapitated, and their brains removed and submerged into oxygenated ice-cold sucrose-substituted artificial cerebrospinal fluid (ACSF) of pH 7.4 (in mM): 240 sucrose, 2.0 KCl, 1 $MgCl_2$, 2 $MgSO_4$, 1 $CaCl_2$, 1.25 NaH_2PO_4, 26 $NaHCO_3$ and 10 glucose. Coronal brain slices were cut at

300 µm using a vibrating microtome (Leica VT 1000S) and allowed to recover at room temperature in a submersion holding chamber with artificial cerebral spinal fluid (ACSF) (in mM): 124 NaCl, 2.5 KCl, 2 $MgCl_2$, 2 $CaCl_2$, 1.25 NaH_2PO_4, 26 $NaHCO_3$, and 17 D-glucose bubbled with 95% O_2 with 5% CO_2.

Whole-cell recordings were made from pyramidal neurons in area CA2, which were identified visually using differential interference contrast (DIC) optics (CA2 neurons were verified in earlier, separate experiments using a CA2-specific fluorescent reporter mouse line (5)). Glass borosilicate pipettes were filled with a potassium gluconate internal solution (in mM) 120 K-gluconate, 10 KCl, 3 $MgCl_2$, 0.5 EGTA, 40 HEPES, 2 Na_2-ATP, 0.3 Na-GTP, pH 7.2), with a tip resistance between 3-4.5 MOhms. Data were collected using Clampex 10.4 and analyzed using Clampfit software (Axon Instruments). Series and input resistances were monitored by measuring the response to a 10mV step at each sweep and cells were included for analysis if <30% change in series and input resistance. Recordings were not compensated for series resistance. Cells were included for any recording lasting more than 15 minutes post LTP-pairing.

To assess excitatory transmission in P14-18 slices, whole-cell recordings were performed in voltage-clamp mode, and postsynaptic currents (PSCs) were evoked with a bipolar stimulating electrode placed in the SR. Excitatory PSCs (EPSCs) were isolated using the $GABA_A$ receptor antagonist bicuculline (10 µm) in the bath solution. Paired-pulse facilitation (PPF) was assessed under similar conditions. Traces presented in Figures 2 and 3 are the average of 4 responses. Inhibitory transmission was not blocked in P8-11 slices because pilot experiments with bicuculline in the bath solution resulted in epileptiform activity during recordings. To determine action potential threshold, whole-cell recordings were performed in current-clamp mode. Current pulses of 180 ms in 0.2 nA steps were delivered and the membrane potential at which the cells first fired action potentials was measured. For long-term potentiation (LTP) experiments, baseline EPSCs were collected every 15 seconds for at least 5 minutes after which a pairing protocol was used, consisting of 1.5 minutes of 3 Hz presynaptic stimulation (270

pulses) paired with postsynaptic depolarization to 0 mV in voltage-clamp mode (10, 11). Data were averaged and normalized to baseline. Methods for LTP experiments using chondroitinase-treated hippocampal slices are detailed in Carstens et al. 2016 (5). In brief, slices were incubated in ACSF with 0.05 U/ml chondroitinase ABC (ChABC, Sigma-Aldrich C3667) for ≥2 h until they were transferred to a recording chamber and continuously bathed in normal ACSF. Hippocampal slices were arbitrarily assigned to chondroitinase treatment group.

Electrode implantation: A P40 Kv1.1 null mouse was implanted with an electrode wire bundle for *in vivo* electrophysiology recordings to measure potential ictal activity. The mouse was anesthetized with ketamine (100mg/kg, IP) and xylazine (7mg/kg, IP) and placed in a stereotaxic apparatus. An incision was made in the scalp and a hole was drilled over the target region for recording. One ground screw was positioned approximately 4 mm posterior and 2 mm lateral to Bregma over the right hemisphere. The electrode was lowered and implanted in the left dorsal hippocampus targeting CA3 (-2.06 AP, -2.2 ML, -2.1 DV from Bregma). The electrode consisted of one bundle of 8 stainless steel wires (44-µm) with polyimide coating (Sandvik Group, Stockholm, Sweden). The wires were then connected to a printed circuit board (San Francisco Circuits, San Mateo, CA), which was connected to a miniature connector (Omnetics Connector Corporation, Minneapolis, MN). Electrode placement was confirmed via wire bundle tracks during histological analysis.

In vivo electrophysiology data acquisition: Five days following electrode implantation, the null mouse underwent electrophysiological recording in the awake, behaving state for a duration of one hour on two consecutive days, and local field potential (LFP) data were analyzed for bouts of ictal activity. Electrographic seizure activity was characterized by large amplitude population spikes, polyspikes and burst activity patterns that reversed in polarity during the course of the seizure and terminated in post-

ictal depression (13). Neural activity was transmitted via a 32-channel wireless 10x gain headstage (Triangle BioSystems International, Durham, NC) and was acquired using the Cerebus acquisition system (Blackrock Microsystems, Salt Lake City, UT). Continuous LFP data were band-pass filtered at 0.3-500 Hz and stored at 1,000 Hz. Neurophysiological recordings were referenced to a silver wire connected to the ground screw.

Chemogenetics: To chemogenetically manipulate CA2 activity, Cre-dependent AAVs encoding either excitatory Gq-coupled or inhibitory Gi-coupled Designer Receptors Exclusively Activated by Designer Drugs (DREADDs) were infused into hippocampi of adult *Amigo2-icre*ERT2+ or *Amigo2-icre*ERT2- mice. Mice were group housed until the time of the AAV infusion, at which point they were singly housed and monitored during recovery from surgery.

Animal numbers: WFA staining intensity was quantified to measure changes in response to chemogenetic changes in activity. Sample sizes for histological analysis are consistent with those used in the field.

Mice	**Infusion hM3Dq**	**Infusion hM4Di**	**No virus infusion**
*Amigo2-icre*ERT2+	(4 mice)	(6 mice)	1
*Amigo2-icre*ERT2-	(4 mice)	(6 mice)	1

In vivo chemogenetics: Gq- or Gi-coupled DREADD AAV (hSyn-DIO-hM3D(Gq)-mCherry or hSyn-DIO-hM4D(Gi)-mCherry, respectively; serotype 5) was delivered to hippocampus near CA2 in *Amigo2-icre*ERT2 mice to selectively target CA2 pyramidal neurons. Expression of each DREADD virus was validated previously using the mCherry reporter that is encoded in the AAV construct (3, 4). The mCherry expressing cells also expressed the CA2 marker PCP4. Viruses listed above were obtained from the viral vector core at the University of North Carolina at Chapel Hill. To prepare mice for the virus-infusion, mice were anesthetized with ketamine (100 mg/kg, IP) and xylazine (7 mg/kg, IP) and placed in

a stereotaxic apparatus. An incision was made in the scalp and a hole was drilled over the CA2 target region for AAV infusion. A 27-gauge cannula connected to a Hamilton syringe was lowered into the hippocampus (in mm: -2.3 AP, +/-2.5 ML, -1.9 mm DV from bregma). Virus was infused unilaterally on the left side for hM3Dq and bilaterally for hM4Di AAV at a rate of 0.1 µl/min for a total of 0.5 µl. The cannula was then left in place for an additional 10 min before removing. Once removed, the scalp was sutured and animals were returned to their cages. Animals were administered buprenorphine (0.1 mg/kg, SQ) for pain preoperatively.

Protocol timeline: After *Amigo2-icre*ERT2+ and *Amigo2-icre*ERT2- adult mice were infused with Gq or Gi-coupled DREADD AAV, the animals recovered from surgery for 2 weeks. The mice were given daily treatments of tamoxifen (100 mg/kg, IP) for 7 days. One week after the last tamoxifen injection, after sufficient time to allow expression of the receptors, the mice were administered the DREADD ligand ("designer drug") clozapine N-oxide (CNO) subcutaneously (1 mg/kg for Gq DREADD infused mice and 5 mg/kg for Gi DREADD infused mice) twice daily (at 10:00 AM and 2:00 PM) for four days. On the fifth day, mice received one CNO treatment (at 10:00 AM) and were perfused for histology 2 hours later. DREADD expression was indeed only expressed in CA2 pyramidal neurons and not in inhibitory neurons, as validated previously in our lab with a Cre-dependent reporter mouse (3, 4). All mice received the viruses and CNO, but only the Cre+ animals expressed the DREADDs.

Statistics: All experiments and analyses were performed by experimenters blinded to genotype and/or treatment groups. Statistical analyses were performed using GraphPad Prism 8 software (Version 8.2.1). Comparisons between groups were analyzed using two-tailed unpaired t-tests and multi-group comparisons were analyzed using 2-way ANOVA with *post-hoc* tests noted by experiments (Bonferroni/ Sidak's/ Tukey's) for pairwise comparisons. Analyses were corrected for repeated measures when

appropriate. P-value and confidence level of <0.05 (95% confidence interval) was considered significant.

Unless otherwise noted, data represent mean ± S.E.M.

Methods References

1. Guy J, Hendrich B, Holmes M, Martin JE, and Bird A. A mouse Mecp2-null mutation causes neurological symptoms that mimic Rett syndrome. *Nat Genet.* 2001;27(3):322-6.
2. Ribeiro MC, and MacDonald JL. Sex differences in Mecp2-mutant Rett syndrome model mice and the impact of cellular mosaicism in phenotype development. *Brain Res.* 2020;1729:146644.
3. Alexander G, Brown L, Farris S, Lustberg D, Pantazis C, Gloss B, et al. CA2 neuronal activity controls hippocampal oscillations and social Behavior. *bioRxiv.* 2017.
4. Alexander GM, Brown LY, Farris S, Lustberg D, Pantazis C, Gloss B, et al. CA2 neuronal activity controls hippocampal low gamma and ripple oscillations. *eLife.* 2018;7.
5. Carstens KE, Phillips ML, Pozzo-Miller L, Weinberg RJ, and Dudek SM. Perineuronal Nets Suppress Plasticity of Excitatory Synapses on CA2 Pyramidal Neurons. *J Neurosci.* 2016;36(23):6312-20.
6. Gong S, Yang XW, Li C, and Heintz N. Highly efficient modification of bacterial artificial chromosomes (BACs) using novel shuttle vectors containing the R6Kgamma origin of replication. *Genome Res.* 2002;12(12):1992-8.
7. Madisen L, Zwingman TA, Sunkin SM, Oh SW, Zariwala HA, Gu H, et al. A robust and high-throughput Cre reporting and characterization system for the whole mouse brain. *Nat Neurosci.* 2010;13(1):133-40.
8. Smart SL, Lopantsev V, Zhang CL, Robbins CA, Wang H, Chiu SY, et al. Deletion of the K(V)1.1 potassium channel causes epilepsy in mice. *Neuron.* 1998;20(4):809-19.
9. Schindelin J, Arganda-Carreras I, Frise E, Kaynig V, Longair M, Pietzsch T, et al. Fiji: an open-source platform for biological-image analysis. *Nat Methods.* 2012;9(7):676-82.
10. Gustafsson B, Wigstrom H, Abraham WC, and Huang YY. Long-term potentiation in the hippocampus using depolarizing current pulses as the conditioning stimulus to single volley synaptic potentials. *J Neurosci.* 1987;7(3):774-80.
11. Malenka RC, and Nicoll RA. NMDA-receptor-dependent synaptic plasticity: multiple forms and mechanisms. *Trends Neurosci.* 1993;16(12):521-7.
12. Farris S, Ward JM, Carstens KE, Samadi M, Wang Y, and Dudek SM. Hippocampal subregions express distinct dendritic transcriptomes that reveal differences in mitochondrial function in CA2. *Cell Rep.* 2019;29(2):522-39 e6.
13. Riban V, Bouilleret V, Pham-Le BT, Fritschy JM, Marescaux C, and Depaulis A. Evolution of hippocampal epileptic activity during the development of hippocampal sclerosis in a mouse model of temporal lobe epilepsy. *Neuroscience*. 2002;112(1):101-11.

Supplemental Figure legends

Supplemental Figure 1

To conditionally delete *Mecp2* from CA2 neurons, we crossed *Amigo2-Cre*$^{+}$ mice with a Cre-dependent *Mecp2* mouse line, floxed- *Mecp2* (*Mecp2*$^{flox/x}$). **A)** Staining for the MeCP2 protein (green) is strongly reduced from CA2/3 neurons and is attenuated in DG cells of the *Amigo2-Cre*$^{+}$; *Mecp2*$^{flox/y}$ mouse. The PNN marker WFA (green) is increased in CA2 in the *Amigo2-Cre*$^{+}$; *Mecp2*$^{flox/y}$ mouse compared with Cre-negative littermates (*Amigo2-Cre*$^{-}$; *Mecp2* $^{flox/y}$). CA2 neurons are labelled with an antibody against RGS14 (red). Scale bars= 200 µm. **B)** Quantification of WFA fluoresence in *Amigo2-Cre*$^{+}$; *Mecp2*$^{flox/y}$ hippocampus compared with controls, Cre- wildtype, Cre+ wildtype, *Amigo2-Cre*$^{-}$; *Mecp2*$^{flox/y}$. WFA fluorescence intensity is significantly greater in the *Amigo2-Cre*$^{+}$; *Mecp2*$^{flox/y}$ mouse in CA2 compared with controls, ***P < 0.0001, one-way ANOVA, Tukey for *post-hoc* test, (N= 3 per group). PNN+ neuron staining intensity in regions CA1 and CA3 were not significantly different, P>0.05, Tukey *post-hoc* test.

Supplemental Figure 2

Excitatory transmission at *Mecp2*$^{-/y}$ and WT CA2 synapses is similarly enhanced by blocking inhibition with 10 µM bicuculline at P14-18. Excitatory postsynaptic current amplitudes in response to indicated stimulation intensity are enhanced at higher stimulation intensities in the presence of the inhibitory blocker bicuculline (+Bic) at WT CA2 synapses (left, P=0.2503 at 600µA stimulus intensity, two-way ANOVA, repeated measures, Sidak's post-hoc analysis, n=7 and 8, -Bic and +Bic respectively) and *Mecp2*$^{-/y}$ CA2 synapses (middle, P=0.1240 at 600µA stimulus intensity, two-way ANOVA, repeated measures, Sidak's post-hoc analysis, n=13 and 8, -Bic and +Bic respectively) compared to no bicuculline (-Bic). Fold change of EPSC amplitude (averaged across stimulation intensities) in the presence and absense of inhitory blocker was not significantly different between *Mecp2*$^{-/y}$ and WT CA2 synapses (P= 0.1163, two-tailed unpaired t-test). Paired-pulse ratio does not differ between *Mecp2*-null and WT CA2 synapses at P14-18, P>0.05 (S1= peak of first stimulus response, S2= peak of second stimulus response).

Supplemental Figure 3

A) Protein levels of the CA2 plasticity-suppressor, RGS14, in area CA2 of *Mecp2*$^{-/y}$ mice compared to WT littermates using immunofluorescence. No significant difference was observed when comparing *Mecp2* knockout across all ages with an ANOVA, however *a priori* post-hoc analysis revealed significantly greater staining intensity of RGS14 fluorescence at P11 in the *Mecp2*-null mice compared with WT (*p=0.0169, unpaired t-test, N= 5 and 4, WT and *Mecp2*-null respectively).

B) The PNN marker WFA is unchanged in areas CA1 and CA3 of *Amigo2-Cre+* mice expressing Gi DREADD or Gq DREADD in CA2 pyramidal neurons compared to control *Amigo2-Cre-* mice (P > 0.05, one-way ANOVA, Tukey's post-hoc test for pairwise comparison, n=5, 6, 4, 5 for Cre- Gi, Cre+ Gi, Cre-Gq, Cre+Gq, respectively). WFA fluorescence intensity was significantly increased in an area of overlying somatosensory cortex of *Amigo2-Cre+* mice expressing Gq DREADD (**P=0.0012, one-way ANOVA, , Tukey *post hoc* test), but not in *Amigo2-Cre+* mice expressing Gi DREADD compared to control *Amigo2-Cre-* mice.

Supplemental Figure 1

PNNs in CA2 are increased in a targeted deletion of *Mecp2* in CA2

A Conditional knockout mouse: *Amigo2-Cre+/-*; *Mecp2*$^{flox/y}$

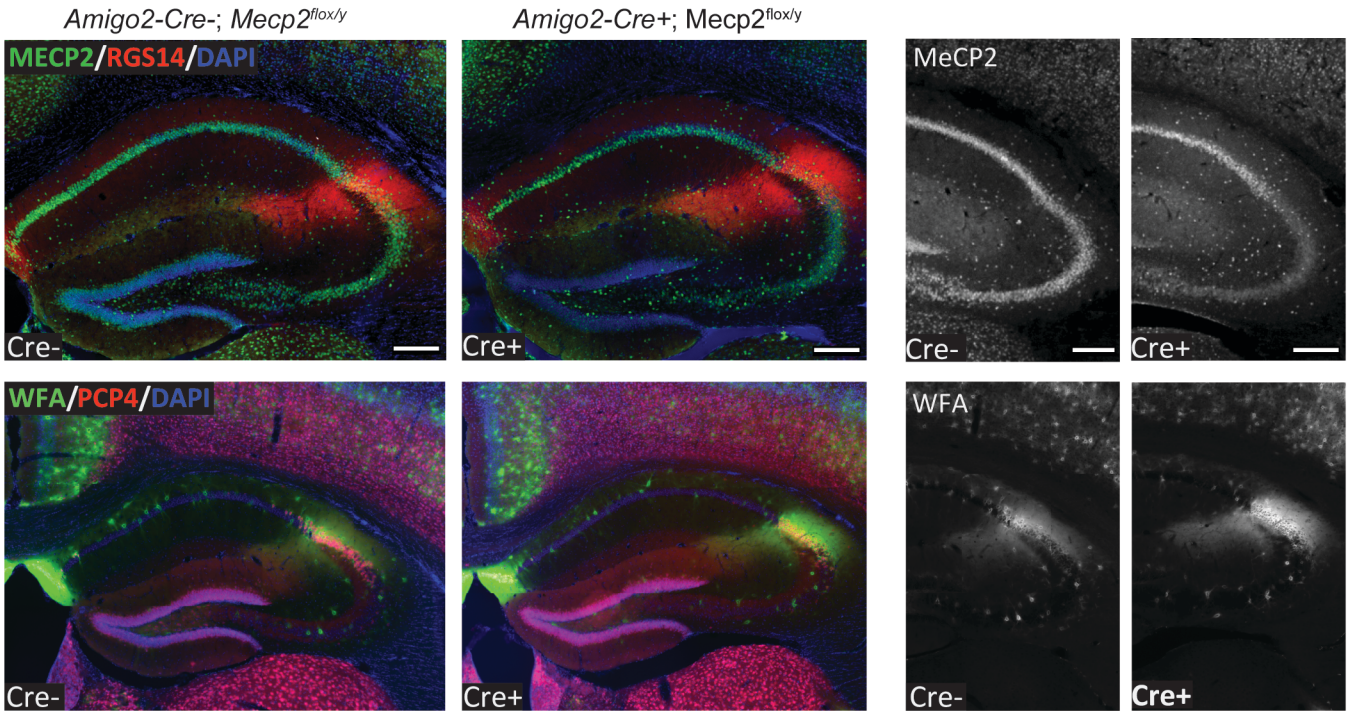

B

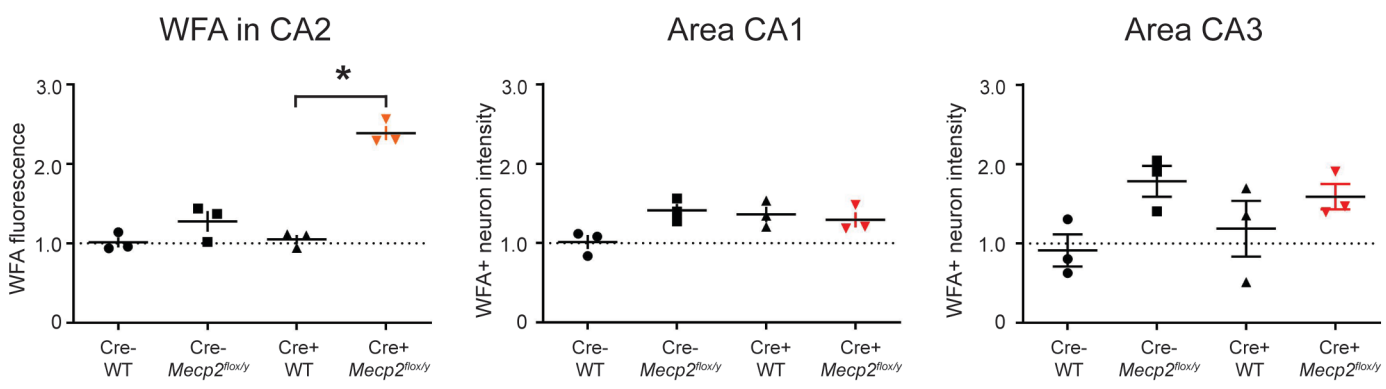

Supplemental Figure 2

Excitatory transmission at CA2 synapses of *Mecp2*-null and WT mice are similarly enhanced by blocking inhibition (P14-18).

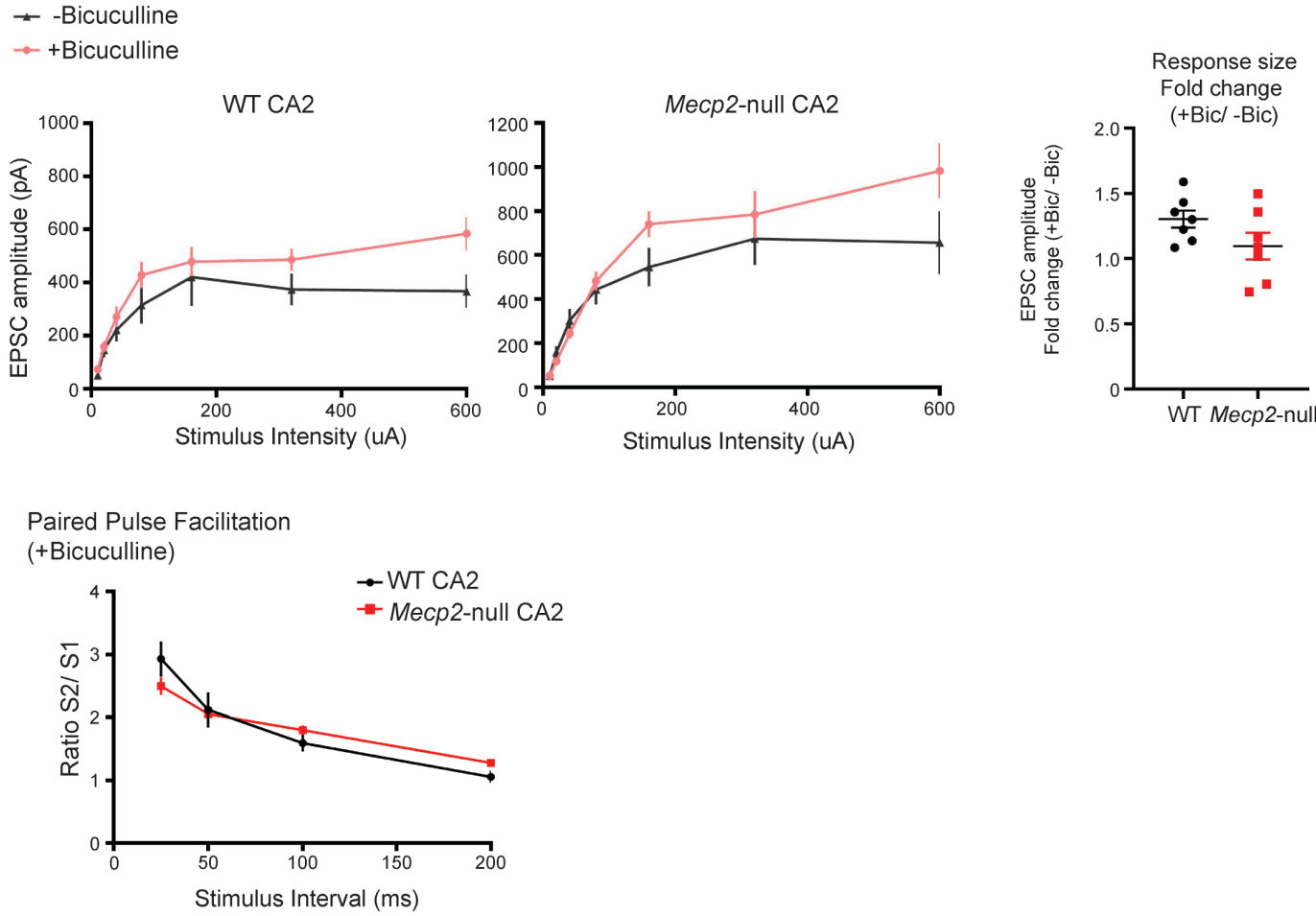

Supplemental Figure 3

A RGS14 protein is increased at P10 in Mecp2-null CA2

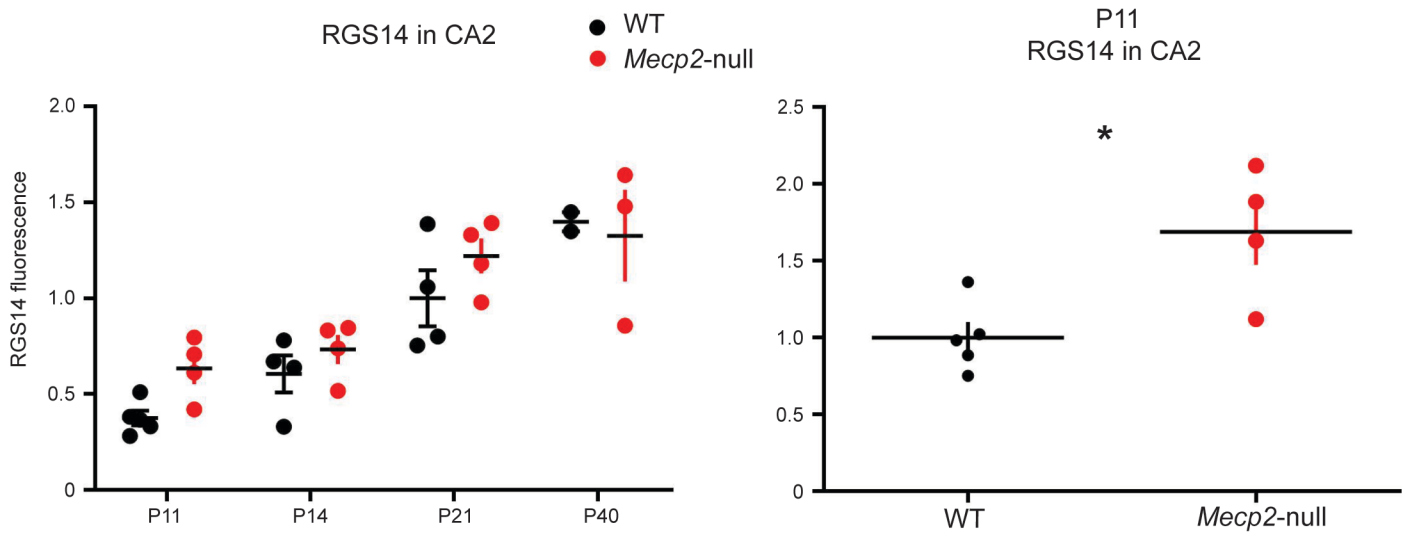

B CA2 chemogenetic activity has no effect on WFA staining intensity in PNN+ neurons in CA1 and CA3.

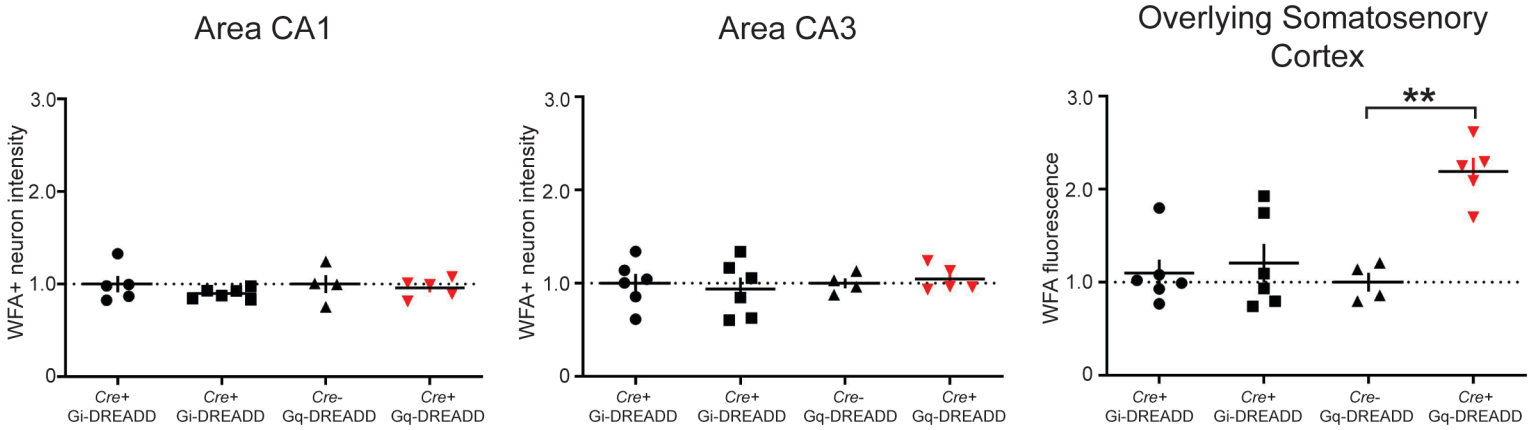

Table 1

	RMP (mV)	Cm (pF)	Ri (Mohm)	AP threshold (mV)	*n* cells (N mice)
P8-11 CA2 WT	-65.22 (0.761)	136.9 (5.337)	305.0 (12.20)	-20.8 (1.907)	60 (14)
P8-11 CA2 *Mecp2*-null	-65.06 (0.747)	145.3 (6.917)	294.1 (16.30)	-16.32 (1.46)	36 (12)
P14-18 CA2 WT	-65.64 (1.649)	179.8 (12.26)$^{+++}$	168.1 (15.84) $^{++++}$	-16.29 (1.85)	17 (7)
P14-18 CA2 *Mecp2*-null	-63.08 (0.875)	181.6 (7.455)	205.9 (8.931)*	-12.90 (1.192)	50 (8)
+ChABC P8-11 CA2 *Mecp2*-null	-61.00 (1.129)	144.8 (7.726)	297.1 (16.50)	N/A	19 (6)
Untreated P8-11 CA2 *Mecp2*-null	-64.40 (1.436)	123.1 (6.139)*	314.7 (21.73)	N/A	19 (4)

Table 1- CA2 intrinsic cell properties were measured in three separate experimental cohorts (seprated by bold lines), each statistically analyzed using a two-tailed unpaired t-test. Resting membrane potential (RMP) and action potential (AP) threshold do not differ in the three experimental groups, P>0.05. Capacitance (C_m) does not differ by genotype at P8-11 or P14-18. C_m increases by age in CA2 controls ($^{+++}$P=0.0006) and R_i decreases by age in CA2 controls, lower in P14-18 compared to P8-11 ($^{++++}$P<0.0001). In chondroitinase (ChABC) treated slices, C_m is higher in *Mecp2*-null CA2 cells compared to untreated *Mecp2*-null slices (*P=0.0378). Input resistance (R_i) does not differ by genotype at P8-11, but *Mecp2*-null animals have a higher R_i compared to WT at P14-18 (*P=0.0412). Indicated is the mean ± SEM. Voltage threshold to fire AP minus RMP.

Figure 5: Raw western blots

Blot A

700 channel:

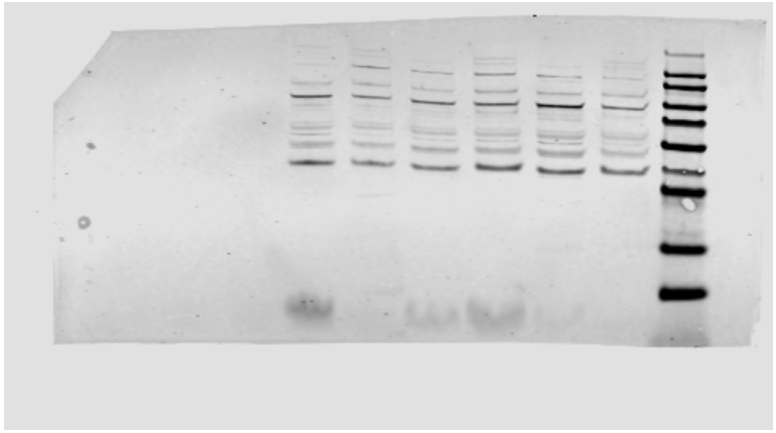

Blot B

700 channel:

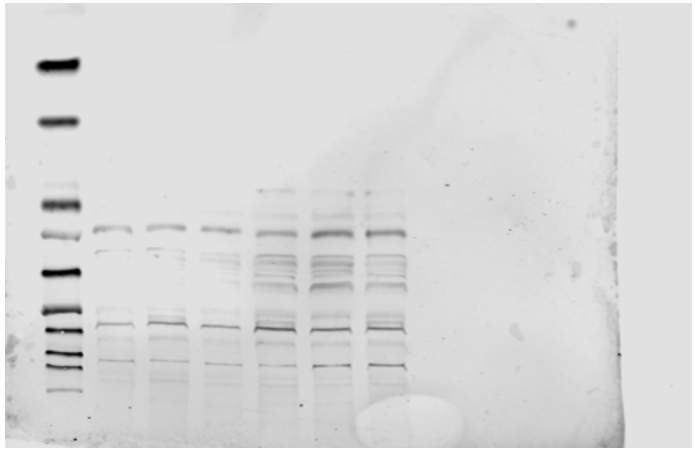

800 channel:

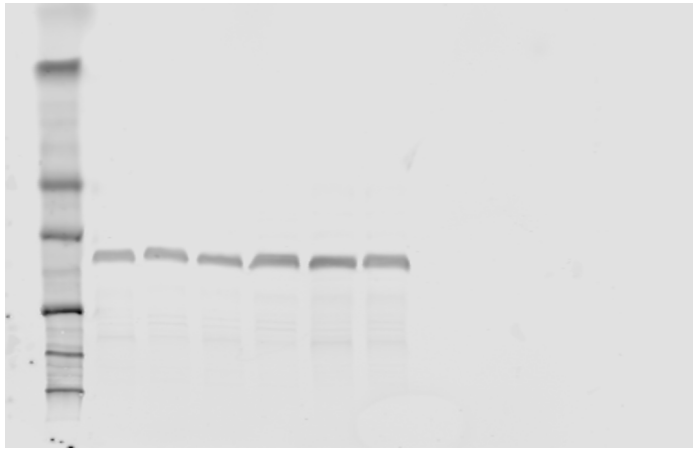

Overlay 700/800 channel:

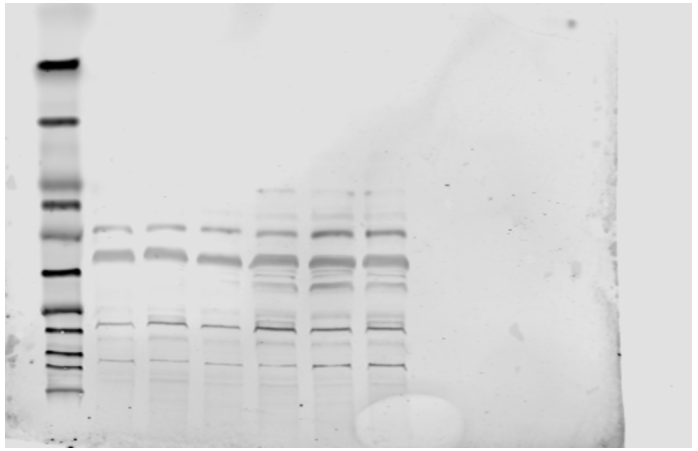

Carstens et. al. 2021

Blot A annotated:

700 channel

MMP9 (rabbit, 1:500) secondary 1:10,000 rabbit 680 (92 kDa)

B-actin (rabbit, 1:10,000) secondary 1:10,000 rabbit 680 (42 kDa)

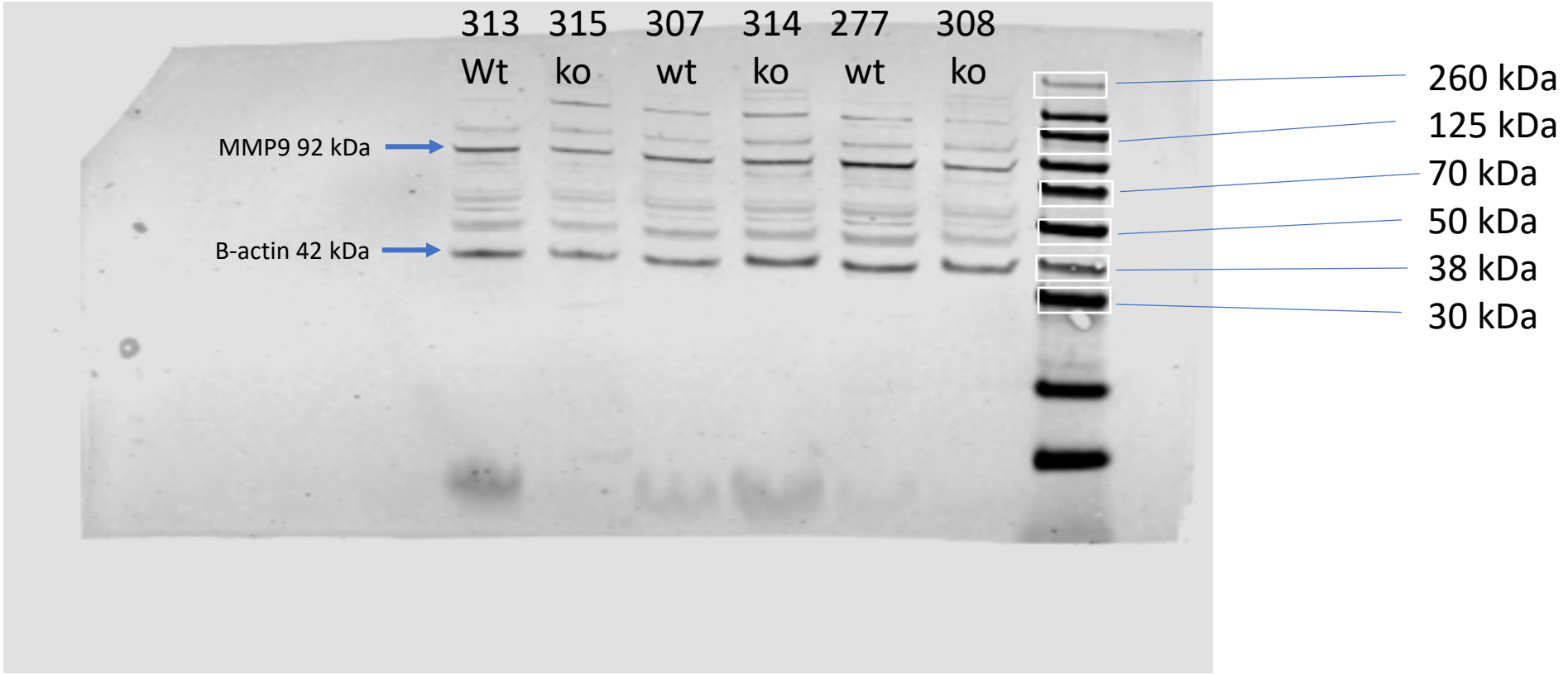

Carstens et. al. 2021

Blot B annotated:

Overlay 700/ 800 channels:

MMP9 (rabbit, 1:500) secondary 1:10,000 rabbit 680 (92 kDa)

B-actin (mouse, 1:10,000) secondary 1:10,000 anti-ms 800 (42 kDa)

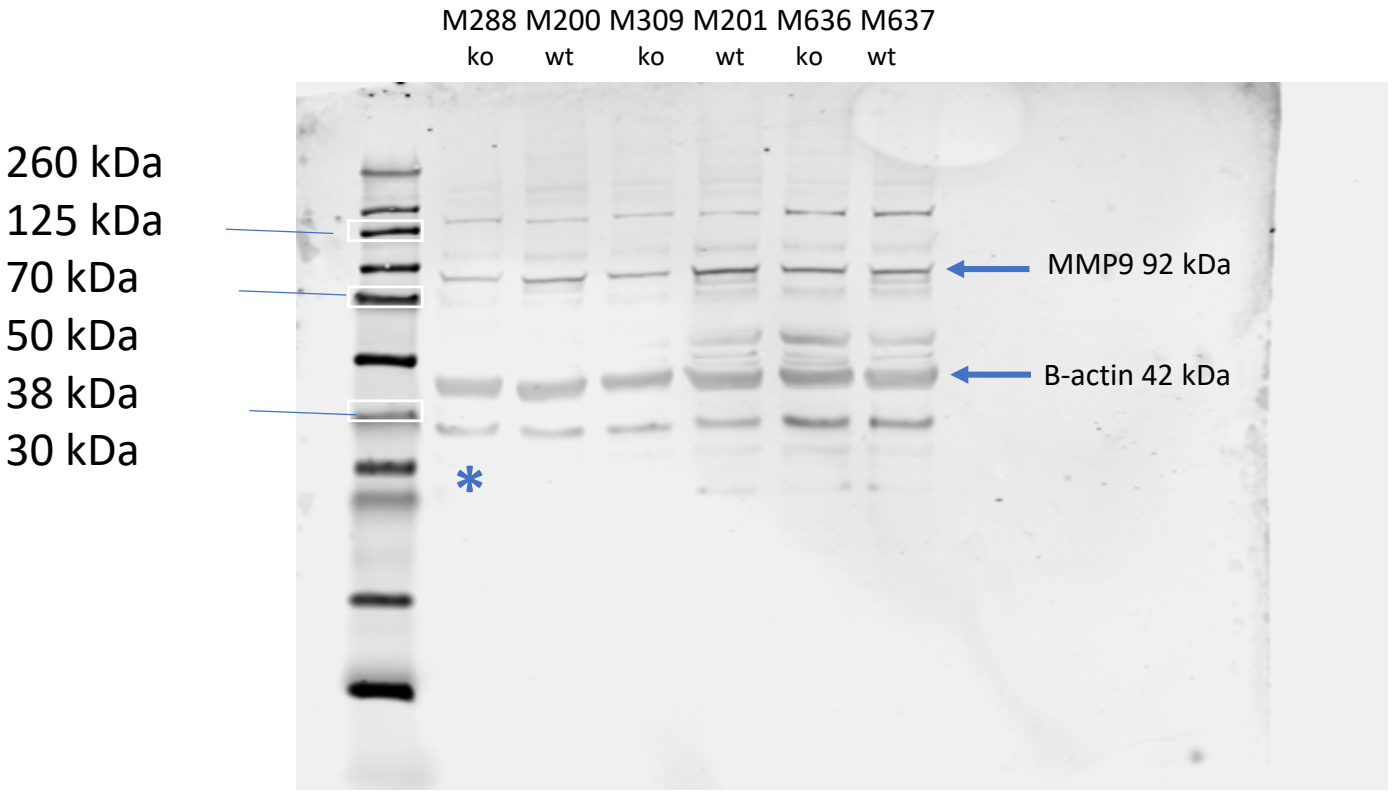

*Cropped this column to the right side to align with WT/KO sequence in Figure 5

700 channel (MMP9 and Mecp2):

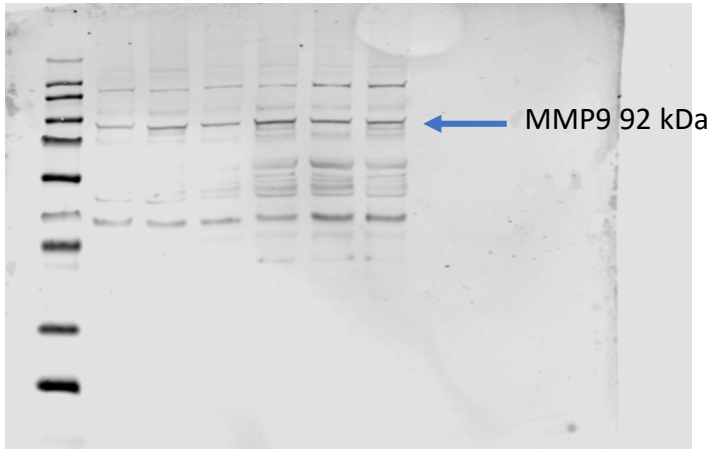

800 channel (B-actin):

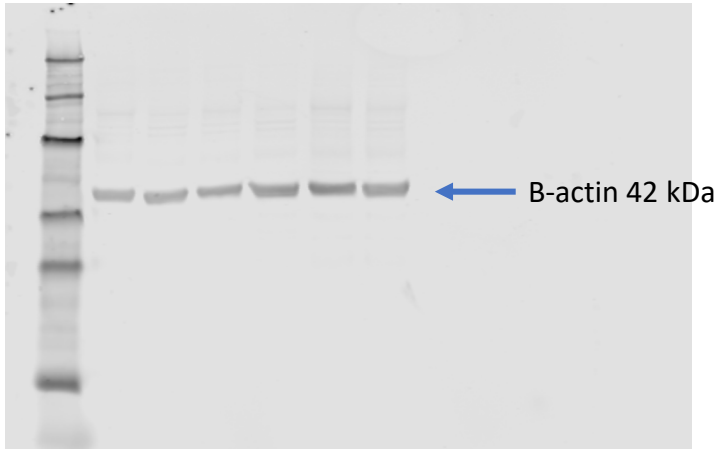

Carstens et. al. 2021